A Geometrical Approach to the Incompatible Substructure Problem in Parallel Self-Assembly

Navneet Bhalla[1], Dhananjay Ipparthi[2], Eric Klemp[3], and Marco Dorigo[2]

[1] Cornell University, Ithaca, New York, USA
navneet.bhalla@cornell.edu
[2] Université Libre de Bruxelles, Brussels, Belgium
{dhananjay.ipparthi,mdorigo}@ulb.ac.be
[3] University of Paderborn, Paderborn, Germany
eric.klemp@uni-paderborn.de

Abstract. The inherent massive parallelism of self-assembly is one of its most appealing attributes for autonomous construction. One challenge in parallel self-assembly is to reduce the number of incompatible substructures that can occur in order to increase the yield in target structures. Early studies demonstrated how a simple approach to component design led components to self-assemble into incompatible substructures. Approaches have been proposed to reduce the number of incompatible substructures by increasing component complexity (e.g. using mechanical switches to determine substructure conformation). In this work, we show how a geometrical approach to self-assembling target structures from the inside-out eliminates incompatible substructures and increases yield. The advantages of this approach includes the simplicity of component design, and the incorporation of additional techniques to reduce component interaction errors. An experiment using millimeter-scale, 3D printed components is used to provide physical evidence to support our geometrical approach.

Keywords: Self-assembly, parallelism, yield, mesoscale, 3D printing.

1 Introduction

Self-assembly is prevalent throughout nature, and is the basis of construction for a myriad of complex biological structures [10]. Inspired by nature, self-assembly is viewed as an enabling technology for the creation of artificial systems [12]. Self-assembly is the autonomous organization of a set of components, in an environment, into structures without human intervention [16]. However, many aspects of self-assembly require further investigation in order to apply the advantages seen in nature to engineered systems, such as massive parallelism [9].

Parallelism in self-assembly can be exploited in two primary forms: (1) the parallel construction of a single target structure, versus (2) the parallel construction of multiple target structures. In both cases, emerging substructures may be incompatible due to binding mechanisms or geometry. In the latter case, a set

T. Bartz-Beielstein et al. (Eds.): PPSN XIII 2014, LNCS 8672, pp. 751–760, 2014.

of components that can self-assemble into a single target structure may not be suitable for constructing multiple target structures due to newly introduced component interactions [2]. For example, an intuitive approach to designing a set of components that can self-assemble into a target hexagonal structure is to dissect the hexagon into fundamental, triangular components [7]. This simple approach is effective for self-assembling a single target structure in parallel. However, this leads to incompatible substructures (e.g. with two and five components) when constructing multiple target structures in parallel.

Furthermore, the latter case is connected to the yield problem, where the objective is to maximize the number of self-assembled target structures and minimize the amount of waste [12]. Reducing or eliminating the number of incompatible substructures that can occur during the self-assembly process is one approach to improving yield [7]. Here, we present a geometrical approach to the design of components that eliminates incompatible substructures from forming, by directing the self-assembly process to construct a target structure from the *inside-out*. The geometry of components in the context of parallel self-assembly has already been considered [11]. However, in this study the focus was not on the construction of target structures (with defined shape) and yield, but rather on the construction of arrays of components (without defined boundaries).

The following section presents the specific incompatible substructure problem of interest here, and methods for directing the self-assembly process to differentiate our geometrical approach. Next, an overview of our geometrical approach is provided, including the designs of components and their environment, in comparison to the simple approach. A description of an experiment follows, which uses millimeter-scale components fabricated by a 3D printer. Components are confined to the surface of a tray, and placed on an orbital shaker. Magnetism is used to attract and repel components. The results show a statistically significant difference between our geometrical approach and the simple approach, especially as the number of potential substructures grows. We discuss several areas of improvement to our approach as future work. We conclude by summarizing how this work provides physical evidence to support our geometrical approach to the incompatible substructure problem in parallel self-assembly.

2 Background

The seminal work by Hosokawa et al. [7] is used to introduce the incompatible substructure problem. Next, the proposed method for directing the self-assembly process by Hosokawa et al. to address this problem is described. Three additional methods to direct the process are presented to contrast our geometrical approach.

2.1 Incompatible Substructure Problem

An early work with the aim of analyzing the dynamics of self-assembling systems was presented by Hosokawa et al. [7]. The target structure for their study was a regular hexagon. The hexagon was divided into six equilateral triangles, serving

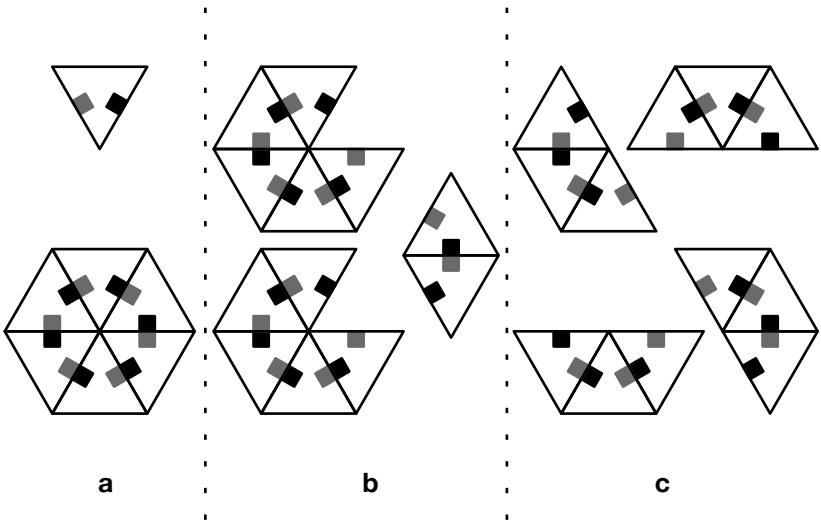

Fig. 1. A triangle component with magnetic north (black) and south (grey) and a target hexagon (a). An example of 12 components for 2 target structures in an intermediate state with incompatible substructures (b) versus compatible substructures (c).

as the base-shape for the centimeter-sized components in their system. Each mechanical component had two permanent magnets, with magnetic north and magnetic south facing outwards on two separate edges (Fig. 1).

With magnetism used to bind components, vibrational energy was used to mix the components. Components were confined to the surface of a rectangular box. The box was oriented vertically, and rotated perpendicularly to its major axis. Misaligned components, errors, could be corrected through component-component/environment interactions due to the vibrations and gravity.

Substructures consisted of one to five components. It is impossible to have incompatible substructures when constructing a single target structure, with the exact number of components. However, when constructing multiple target structures in parallel, incompatible substructures can occur (Fig. 1). Hosokawa et al. calculated the probability of the five types of substructures binding together [7]. Based on these probabilities, they were able to derive a master equation, conceptually similar to chemical kinetics. Their analytical method was used to both calculate yield and understand the dynamics of this system over time.

2.2 Directed Self-Assembly

To improve yield, Hosokawa et al. proposed an alternative set of components to the simple, homogenous set of components [7]. The alternative set exploited conformational switching, a mechanism that changes a feature (e.g. binding mechanism or geometry) of a component based on local component interaction [13].

The alternative set consisted of two types, *seed* and *variable*, components. One seed component is required for each target structure. Permanent magnets of opposite polarity were embedded within two edges of a seed component. However, variable components had two permanent magnets placed within their interior, which would only move to the edge when a magnet of opposite polarity was present in a neighboring component. The use of a seed and variable components created an *assembly sequence*, and eliminated the formation of incompatible substructures. One drawback was that the proposed seed components could self-assemble, resulting in errors (due to magnetic binding and the triangular shape of the components). Hosokawa et al. analytically showed how their conformational switching approach could improve yield over their simple approach [7]. To the best of our knowledge, this system has not been physically implemented.

Additional designs for conformational switching and alternative methods for directing the self-assembly process have been developed. Engineered proteins using ligand switches [4] and robotic modules using electro-mechanical switches [8] have been physically implemented. Synthesized DNA using a nucleic acid switch has been theorized [5]. DNA self-assembly using the abstract Tile Assembly Model, leverages seed tiles, environment temperature, and cooperative binding to direct crystallization [17]. Seed tiles with a larger number of binding sites have been physically demonstrated to improve the yield of algorithmic crystals [1]. Alternatively, the self-assembly process can be divided into time steps, and the set of components at different stages can also be used to direct the process by constructing target structures from the inside-out [2].

There are several drawbacks to theses methods. For the staging method, it becomes an increasingly difficult task to prevent error interactions when increasing the number of components and interdependent stages. Permitting binding at one temperature and preventing binding at another is the biggest challenge in physically implementing systems based on the abstract Tile Assembly Model. Conformational switches are challenging to engineer, and as shown in the next section, unnecessary for self-assembling target structures with basic geometries.

3 Geometrical Approach

We present our geometrical approach to the incompatible substructure problem in parallel self-assembly. The core idea of our approach is that component geometry can direct the self-assembly process, as an alternative to conformational switching, multiple environmental conditions, or staging. A variation to the simple component set, by Hosokawa et al., is used to contrast a component set based on our geometrical approach. This change in geometry directs the target structure to form from the inside-out, instead of the less versatile assembly path generated by the conformational switching approach by Hosokawa et al.

Instead of a regular hexagon, a circle is used as the target structure. This change in target shape reduces the contact surface area between target structures, decreasing the potential for interaction errors and improving the mixing of target structures and substructures. It also allows for the target shape to remain

constant, while being able to vary the number of components with regularity. Scaling the number of divisions of the circle from three (minimum number for incompatible substructures to form) to six allows for deeper investigation.

Mesoscale (micrometer to millimeter) self-assembly offers flexibility in design and functionality that is unparalleled by molecular systems [15]. Millimeter-scale components, fabricated by a 3D printer, are used in this work. The target circle is 25 mm in diameter. Three types of components are used in this work, *sector* (first, homogenous set), and *disc* and *ray* (second, heterogeneous set).

Sector components are similar to the simple set used by Hosokoawa et al. (named after dividing a circle into equal subunits). Sector (S) components are denoted by C_x^S, where $x \in \{3, 4, 5, 6\}$. Instead of embedding two magnets of opposite polarity in the edges, one permanent magnet (polarity north) and a ferromagnetic micro-screw are used (Fig. 2). This reduces misalignment errors by up to 50%, in comparison to the simple component set by Hosokawa et al.

The design of disc and ray components are based on our geometrical approach (named after sunflowers; ray flowers around the middle disc flowers [14]). Disc (D) and ray (R) components are denoted by C_x^D and C_x^R, where $x \in \{3, 4, 5, 6\}$. A ferromagnetic micro-screw is used in each ray, and one permanent magnet (polarity north) is used in each ray location in a disc (Fig. 2). As well, *key-lock* shapes are used to reduce interaction errors [2]. Exploiting symmetry, discs are not magnetically attracted and cannot misalign due to geometry, in comparison to the assembly errors of the seed components by Hosokawa et al. The geometry of these components prevents incompatible substructures from forming.

Sector and disc-ray component sets use identical circular tray environments (similar to petri dishes). The dimensions of a tray include an inner wall diameter of 118.55 mm and height of 6 mm. A tray is fastened horizontally to an orbital

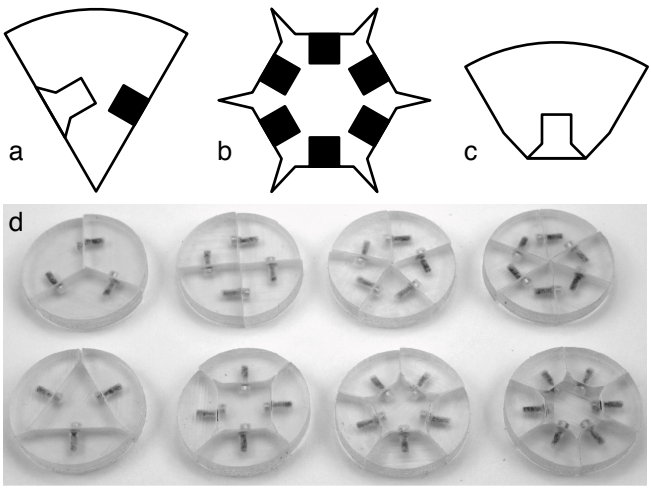

Fig. 2. Abstract examples of C_6^S (a), C_6^D (b), and C_6^R (c), and the 8 types of target structure with 3D printed components embedded with magnets and micro-screws (d)

shaker, providing vibrational energy to the passive, mechanical components; a lid constrains the components to the tray surface. Each tray accommodates 10 target structures. The shaking speed and the tray dimensions are based on preliminary experiments conducted by the authors. Complete physical specifications of the tray, and the sector, disc, and ray components are provided in [3].

4 Experiment

The benefit of our geometrical approach will be shown by a statistically significant difference in yield between the sector and disc-ray component sets. The null hypothesis, H_0, is that there is no difference in the yield of self-assembled circular target structures between the sector and disc-ray component sets. The alternative hypothesis, H_1, is that there is a difference in the yield of self-assembled circular target structures between the sector and disc-ray component sets.

To test H_0, 10 trials of this experiment are conducted. The dependent variable is the number of self-assembled target structures. The independent variable is the set of components. A trial is conducted for C^{S}_{3-6}, and C^{D}_{3-6} and C^{R}_{3-6}. Enough components are provided to self-assemble 10 target structures. The control group is the set of sector components and the experimental group is the set of disc-ray components (subgroups denoted by CG^{S}_{y} and EG^{DR}_{y}, where $y \in \{3, 4, 5, 6\}$).

The structure of all the components is made from a photopolymer resin, fabricated using an Objet Eden 3D printer. Finishing the components includes manually inserting permanent magnets and micro-screws. Four trays are used in the experiment, in order to conduct trials in parallel. The base of each tray is made from ABS plastic, fabricated using a Stratasys Fortus 3D printer. The laser-cut tray lids are made from clear acrylic. A full list of the materials and procedures for constructing the components and trays is provided in [3].

The four trays are fastened to an Excella E5 orbital shaker. At the start of each trial, all the components in a subgroup are randomly placed into one of the four trays (ensuring components are not initially aligned to self-assemble). The shaker is turned on and set to 300 rpm. The shaker is turned off after 300 seconds. A complete description of the experiment procedure is provided in [3]. At the end of each trial, the following four quantitative measurements are recorded: (1) the number of self-assembled target structures, (2) the number and type of compatible substructures, (3) the number and type of incompatible substructures, and (4) the number and type of errors (misalignment and defects).

5 Results

Frequency histograms for the number of self-assembled target structures, for the control and experimental groups, are provided in Fig. 3. The frequency histograms show that the yield in target structures is not normally distributed for both groups. Therefore, the non-parametric Mann-Whitney-U test is used to test H_0 [6]. The sample size, and median and mean number of self-assembled target structures for the control group are 40, 7, and 6, for the experimental

group are 40, 9, and 9. The calculated critical value, U, is 1,394. The difference in yield between the control and experimental groups is statistically significant (two-tailed test, p-value < 0.001). Therefore, we reject H_0.

A deeper investigation illustrates the difference in yield and waste between the subgroups, CG_{3-6}^{S} and EG_{3-6}^{DR}. Here, waste is considered to be any substructure that remains at the end of a trial. The first box-and-whisker plot shows the interquartile range and the minimum and maximum number of self-assembled target structures, yield, for each subgroup (Fig. 3). The second box-and-whisker plot shows the interquartile range and the minimum and maximum number of compatible substructures and incompatible substructures for CG_{3-6}^{S} (Fig. 3). The third box-and-whisker plot shows the interquartile range and the minimum and maximum number of disc-based substructures and the number of single ray components for EG_{3-6}^{DR} (Fig. 3).

Notably, CG_{4}^{S} achieved a consistently high yield, and only had incompatible substructures occur in trials 9 and 10 (substructures with 3, 3, and 2 components for both trials). This high yield might be attributed to symmetry, but requires further investigation. Trials 1 and 2 of CG_{5}^{S} did not have incompatible substructures, and instead had compatible substructures with 3 and 2 components for both trials. For CG_{5}^{S}, trials 3 to 10 did not have any compatible substructures. Only trials 2, 3, and 4 of CG_{6}^{S} had compatible substructures. The typical number of components in the incompatible substructures for CG_{5}^{S} and CG_{6}^{S} were one less than required for the target structures. For trials 1−10, for EG_{3-5}^{DR}, only a single, unattached C_{3-5}^{R} prevented 10 target structures from self-assembling. For EG_{6}^{DR}, trials 1, 5, and 6 had a single C_{6}^{R} each. Trial 3 had one C_{6}^{D} with one empty slot and a second C_{6}^{D} with two empty slots (three C_{6}^{R}). Trials 4, 7, and 9 had two C_{6}^{D} with one empty slot each (two C_{6}^{R}). And, trial 8 had one C_{6}^{D} with two empty slots (two C_{6}^{R}). A larger sample size is required to directly compare CG_{3-6}^{S} to EG_{3-6}^{DR}. Fig. 4 shows examples from the experiment.

No misalignment errors were observed. Only one defect error occurred in trial 4 of EG_{6}^{DR}, where a magnet from C_{6}^{D} dislodged and self-assembled two C_{6}^{R}. Despite this error, the difference in yield between the sector and disc-ray groups is statistically significant. Even when increasing the number of components in a target structure, we attribute this difference to our geometrical approach.

6 Future Work

We are currently investigating three extensions to our approach. First, we are setting-up a camera tracking system to record the physical trials, in order to conduct deeper analysis into the self-assembly process of target structures in parallel. One of the shortcomings of the geometrical approach described here is that it is restricted to a single layer of components. Second, we are investigating new geometries in order to scale the number of components to additional layers, and leverage the new geometries to autonomously stage the construction of each layer from the inside-out. For example, more complex arrangements of multiple permanent magnets can be used to selectively attract and repel a wider variety

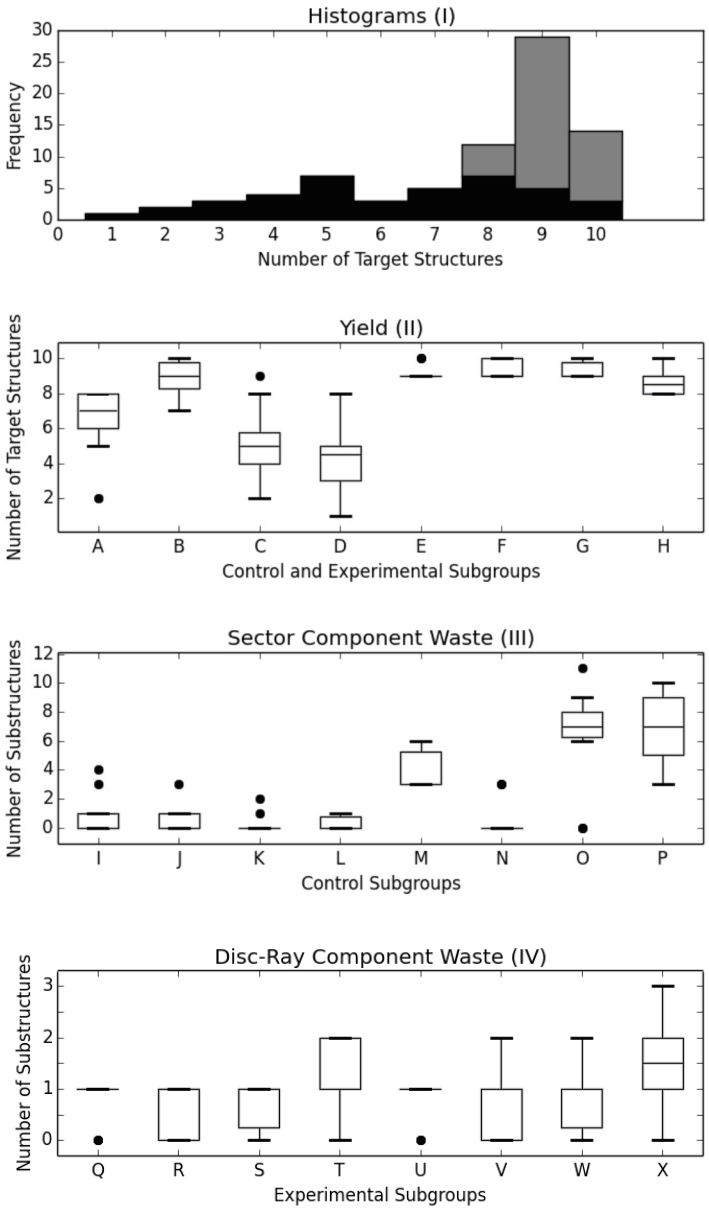

Fig. 3. (I) Histograms for control (black) and experimental (grey) groups. (II) Box-and-whisker plot for the number of self-assembled target structures in 10 trials for CG^{S}_{3-6} (A-D) and EG^{DR}_{3-6} (E-H). (III) Box-and-whisker plot for the number of compatible, CG^{S}_{3-6} (I-L), and the number of incompatible, CG^{S}_{3-6} (M-P), substructures in 10 trials. (IV) Box-and-whisker plot for the number of disc-based substructures, EG^{DR}_{3-6} (Q-T), and the number of single ray components, EG^{DR}_{3-6} (U-X), in 10 trials.

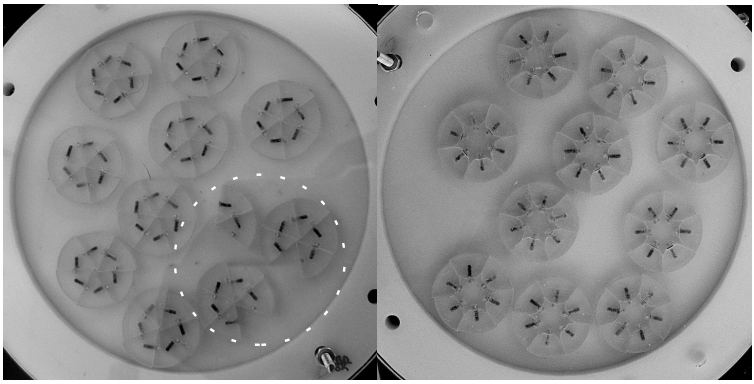

Fig. 4. Example of incompatible substructures (2, 5, and 5 component substructures, CG_6^S, trial 10; left), and of self-assembled target structures (EG_6^{DR}, trial 10; right)

of component types (i.e. components in different layers), while self-assembling structures from the inside-out [2]. Third, we are considering new component and environment designs in order for the components to move and self-assemble in three spatial dimensions.

7 Conclusions

In this work, we presented our geometrical approach to the incompatible substructure problem. The primary contribution of this work is that our approach eliminates incompatible substructures from forming during the self-assembly process. The secondary contributions of this work includes the reduction of component interactions errors by combining a permanent-ferromagnetic binding mechanism with the key-lock principle, and a physical experiment that produced a high yield in target structures (even as the number of components increased) while reducing waste. The evidence from this experiment supports our geometrical approach to the incompatible substructure problem in parallel self-assembly.

Acknowledgments. This work has been partially supported by a Postdoctoral Fellowship provided by the Natural Sciences and Engineering Research Council of Canada, and by the European Research Council through the ERC Advanced Grant "E-SWARM: Engineering Swarm Intelligence Systems" (contract 246939). Marco Dorigo acknowledges support from the Belgian F.R.S.–FNRS. We thank the Direct Manufacturing Research Center and Hamburg University of Applied Sciences for 3D printing the parts used in the experiment.

References

1. Barish, R.D., Schulman, R., Rothemund, P.W.K., Winfree, E.: An information-bearing seed for nucleating algorithmic self-assembly. Proc. Natl. Acad. Sci. U.S.A. 106(15), 6054–6059 (2009)

2. Bhalla, N., Bentley, P.J., Vize, P.D., Jacob, C.: Staging the self-assembly process: Inspiration from biological development. Artificial Life 20(1), 29–53 (2014)
3. Bhalla, N., Ipparthi, D., Klemp, E., Dorigo, M.: A geometrical approach to the incompatible substructure problem in parallel self-assembly: supplementary material. Tech. Rep. TR/IRIDIA/2014-010, IRIDIA, Université Libre de Bruxelles, Brussels, Belgium (2014)
4. Dagliyan, O., Shirvanyants, D., Karginov, A.V., Dinga, F., Feea, L., Chandrasekarana, S.N., Freisingerd, C.M., Smolend, G.A., Huttenlocherd, A., Hahnc, K.M., Dokholyana, N.V.: Rational design of a ligand-controlled protein conformational switch. Proc. Natl. Acad. Sci. U.S.A. 110(17), 6800–6804 (2013)
5. Gautam, V.K., Haddow, P.C., Kuiper, M.: Reliable self-assembly by self-triggered activation of enveloped DNA tiles. In: Dediu, A.-H., Martín-Vide, C., Truthe, B., Vega-Rodríguez, M.A. (eds.) TPNC 2013. LNCS, vol. 8273, pp. 68–79. Springer, Heidelberg (2013)
6. Hettmansperger, T.P., McKean, J.W.: Robust nonparametric statistical methods. Chapman & Hall/CRC Press, Boca Rotan (2010)
7. Hosokawa, K., Shimoyama, I., Miura, H.: Dynamics of self-assembling systems: Analogy with chemical kinetics. Artificial Life 1(4), 413–427 (1994)
8. Klavins, E.: Programmable self-assembly. IEEE Control Systems Magazine 27(4), 43–56 (2007)
9. Mastrangeli, M., Abbasi, S., Van Hoof, C., Celis, J.P., Böhringer, K.F.: Self-assembly from milli- to nanoscales: methods and applications. Journal of Micromechanics and Microengineering 19(8), 1–37 (2009)
10. Mendes, A.C., Baran, E.T., Reis, R.L., Azevedo, H.S.: Self-assembly in nature: using the principles of nature to create complex nanobiomaterials. WIREs Nanomedicine and Nanobiotechnology 5(6), 582–612 (2013)
11. Miyashita, S., Nagy, Z., Nelson, B.J., Pfeifer, R.: The influence of shape on parallel self-assembly. Entropy 11(4), 643–666 (2009)
12. Pelesko, J.A.: Self Assembly: The Science of Things that Put Themselves Together. Chapman & Hall/CRC Press, Boca Rotan (2007)
13. Saitou, K.: Conformational switching in self-assembling mechanical systems. IEEE Transactions on Robotics and Automation 15(3), 510–520 (1999)
14. Schneiter, A.A., Miller, J.F.: Description of sunflower growth stages. Crop Science 21(6), 901–903 (1981)
15. Whitesides, G.M., Boncheva, M.: Beyond molecules: Self-assembly of mesoscopic and macroscopic components. Proc. Natl. Acad. Sci. U.S.A. 99(8), 4769–4774 (2002)
16. Whitesides, G.M., Grzybowski, B.: Self-assembly at all scales. Science 295(5564), 2418–2421 (2002)
17. Winfree, E., Liu, F., Wenzler, L.A., Seeman, N.C.: Design and self-assembly of two-dimensional DNA crystals. Nature 394, 539–544 (1998)